The supplementary data includes:

Supplementary Figs. S1 to S6
Supplementary Tables S1 to S5 (provided as separate excel files)

Supplementary Fig. S1

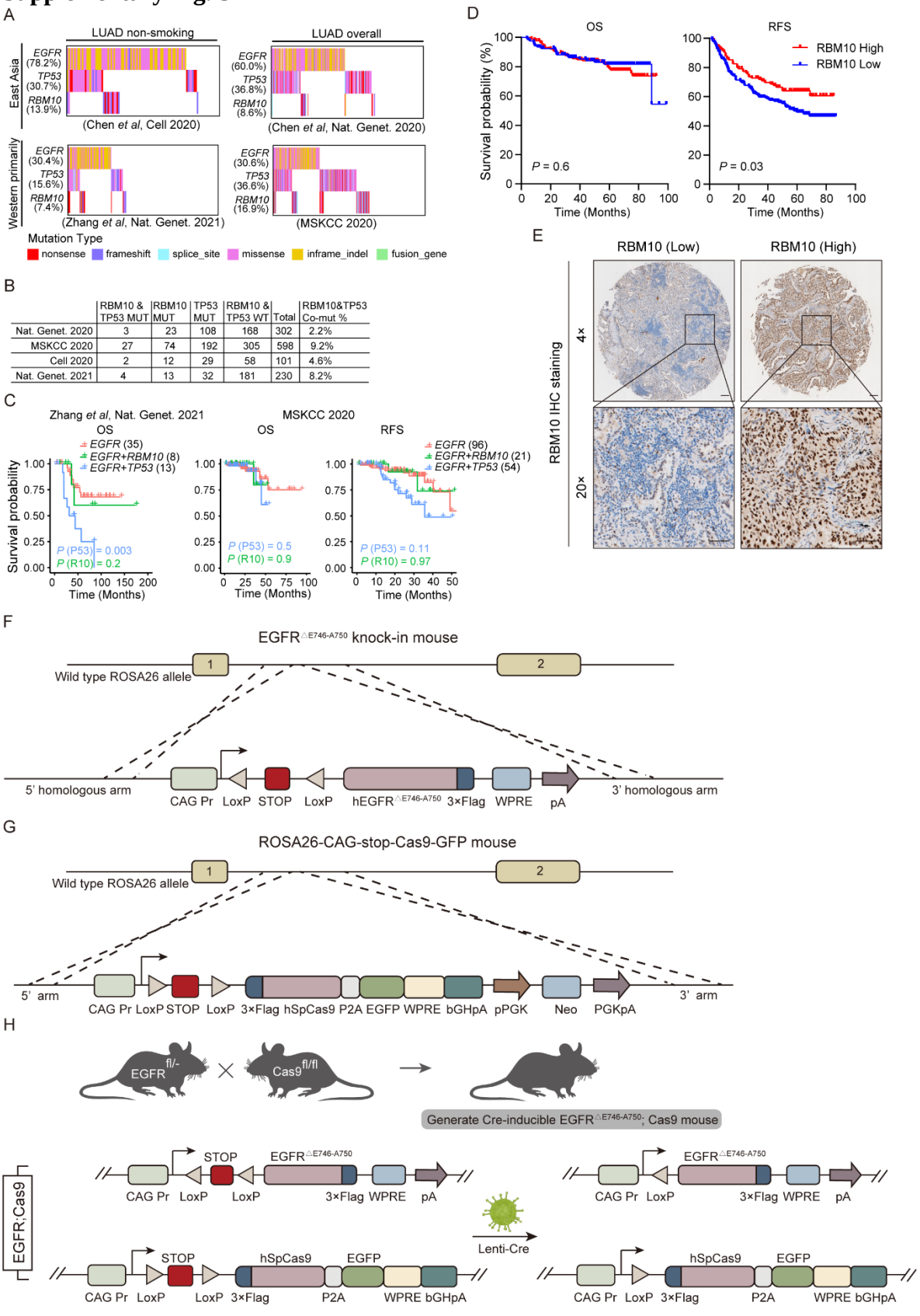

	RBM10 & TP53 MUT	RBM10 MUT	TP53 MUT	RBM10 & TP53 WT	Total	RBM10&TP53 Co-mut %
Nat. Genet. 2020	3	23	108	168	302	2.2%
MSKCC 2020	27	74	192	305	598	9.2%
Cell 2020	2	12	29	58	101	4.6%
Nat. Genet. 2021	4	13	32	181	230	8.2%

Supplementary Figure S1. Mutational spectrum of *EGFR*, *RBM10*, and *TP53* and their correlations with patient survival in lung adenocarcinoma (LUAD), and the construction of *EGFR* knock-in and EGFR; Cas9 mouse model. (**A**) Spectrum and (**B**) data table for *EGFR*, *RBM10*, and *TP53* mutations in different LUAD datasets. The percentage of *RBM10* and *TP53* mutation co-occurrence were shown in data table. (**C, D**) Overall survival (OS) and recurrence free survival (RFS) curve of LUAD patients stratified by *EGFR*, *RBM10*, and *TP53* mutations from the indicated cohorts (C) and by RBM10 expression estimated by immunohistochemistry (IHC) of LUAD tissue microarray (TMA) (D). Number of patients was indicated in parenthesis in (**C**). *P* values were calculated by log-rank tests. (**E**) Representative images of RBM10 immunohistochemistry analysis of TMA LUAD samples, with high or low immunoreactive score (IRS) of RBM10. Scale bar: 100μm for 4×magnification, and 50μm for 20×magnification. (**F-H**) Schematic illustration of the generation of $EGFR^{\triangle E746\text{-}A750}$ knock-in and EGFR; Cas9 mouse model.

Supplementary Fig. S2.

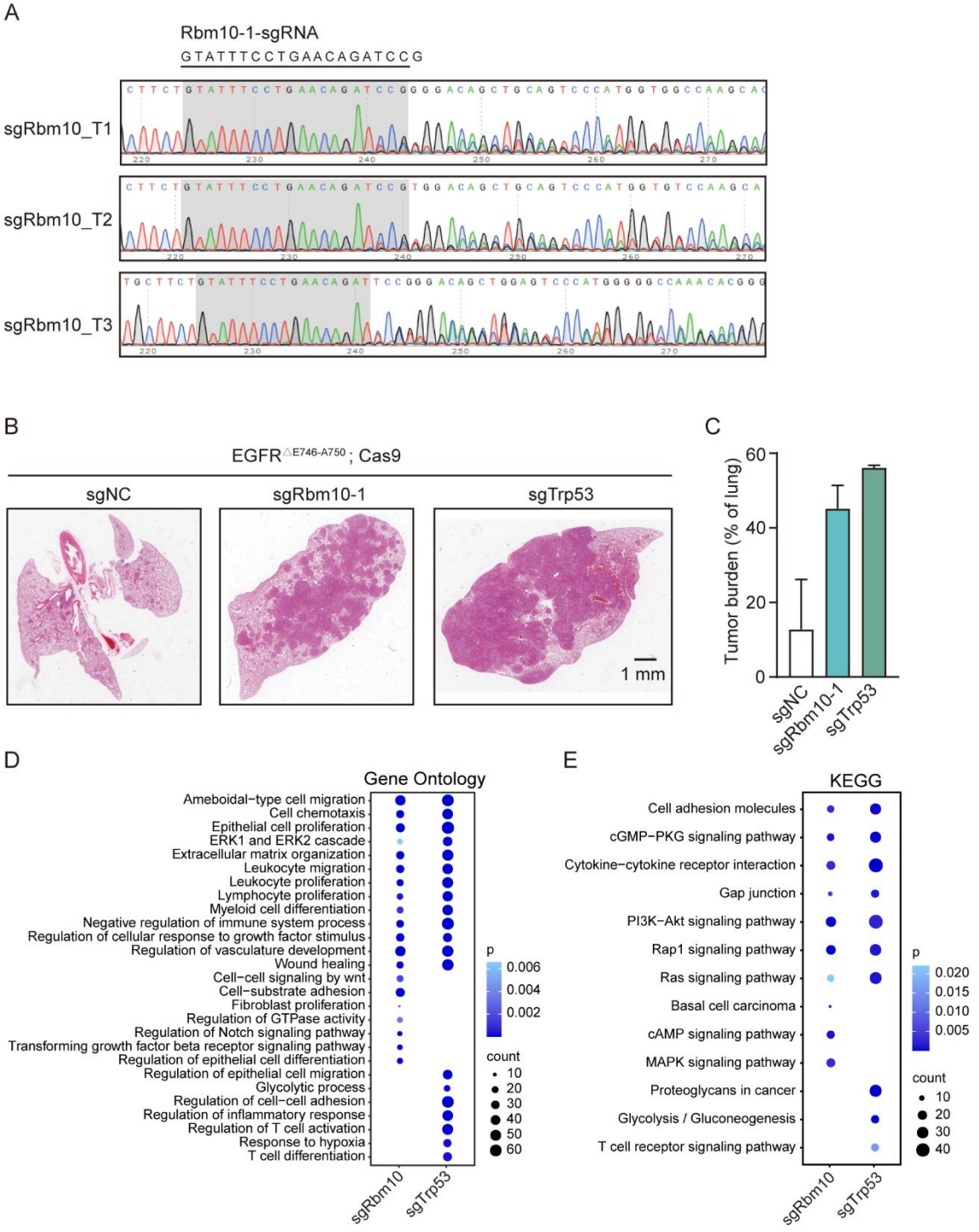

Supplementary Figure S2. sgRNA-mediated *Rbm10* depletion promotes *EGFR*-driven lung tumor development. (**A**) sgRNA-mediated *Rbm10* knockout efficiency confirmed by Sanger sequencing of DNA fragments from mice tumors. (**B, C**) Hematoxylin and eosin (H&E) staining of tumor sections in sgNC, sgRbm10 and sgTrp53 mice. n = 2 biological replicates. Error bars represent ＋SEM. (**D, E**) Dot plot illustration of GO (gene ontology) and KEGG (Kyoto Encyclopedia of Genes and Genomes) enrichment analysis of DEGs indicated in Fig. 2A.

Supplementary Fig. S3.

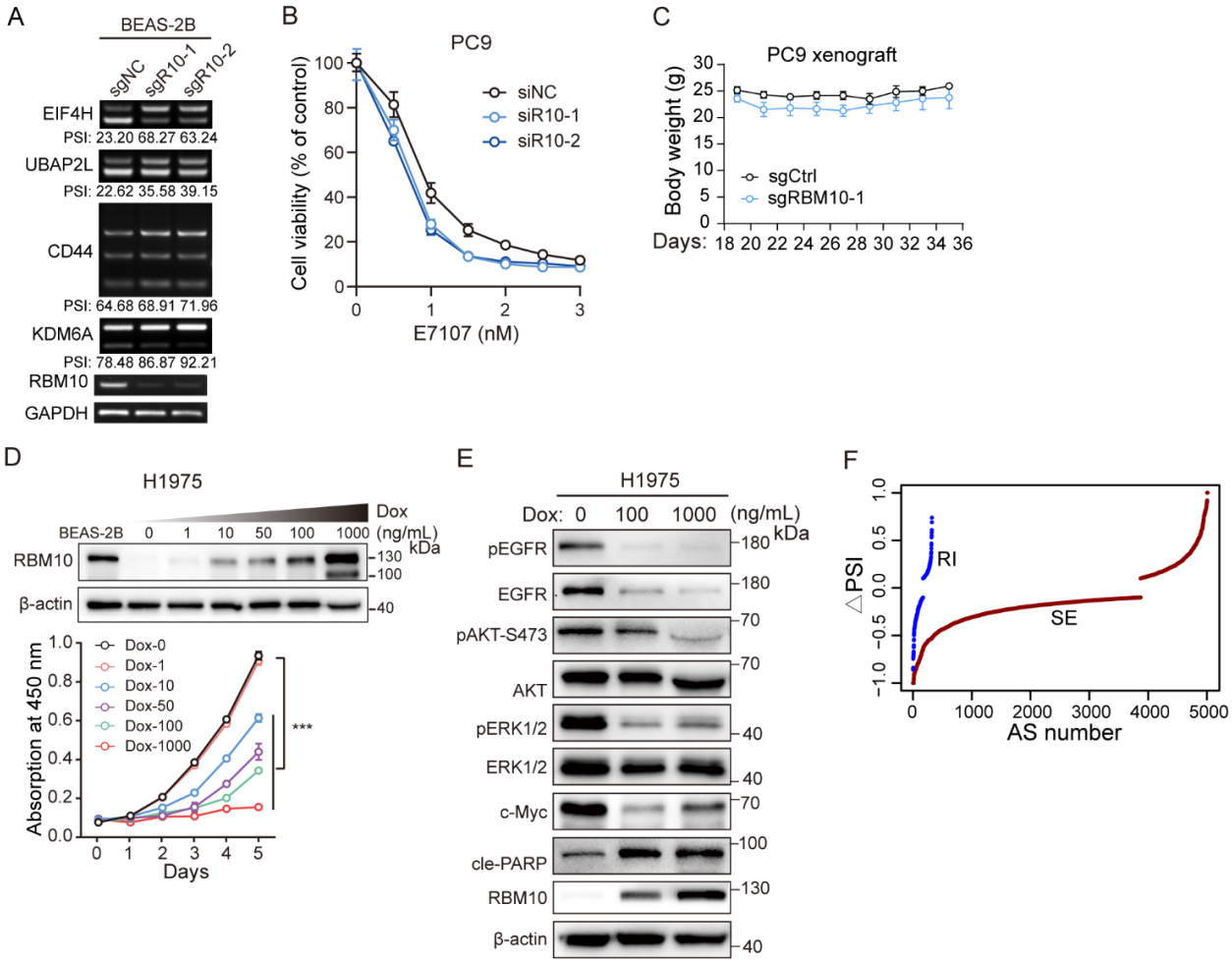

Supplementary Figure S3. Impacts of RBM10 expression on target splicing, response to spliceosome inhibitor and the growth of LUAD cells. (**A**) Confirmation of the splicing changes following *RBM10* knockout using two independent single guide RNAs in BEAS-2B cells. Relative expression of *RBM10* was shown. Loading control: GAPDH. (**B**) Dose-response curves of *RBM10* wild type PC9 LUAD cells treated with E7107 under control and *RBM10* silencing (siNC and siRBM10) conditions, respectively. n = 4 biological replicates. (**C**) Body weight of nude mice upon E7107 treatment, as indicated in Fig. 4D-F. (**D**) Cell growth of *RBM10*-deficient H1975 LUAD cells upon increasing amount of RBM10 re-expression. Dox: Doxycycline. (**E**) Western blot analysis of phosphorylated and total EGFR, AKT, and ERK as well as c-Myc and apoptotic marker protein expression in H1975 cells following RBM10 re-expression. Loading control: β-actin. (**F**) Alternative splicing (AS) changes of PC9 cells treated with Pladienolide B. Cutoff: |△PSI (percent-spliced-in) | ≥ 0.1, *P* value < 0.05. SE: skipped exon, RI: retained intron.
Error bars represent ±SD in (**D**), ±SEM in (**B**, **C**). *** $P < 0.001$, ns: not significant, two-way ANOVA followed by Bonferroni's tests in (**D**).

Supplementary Fig. S4.

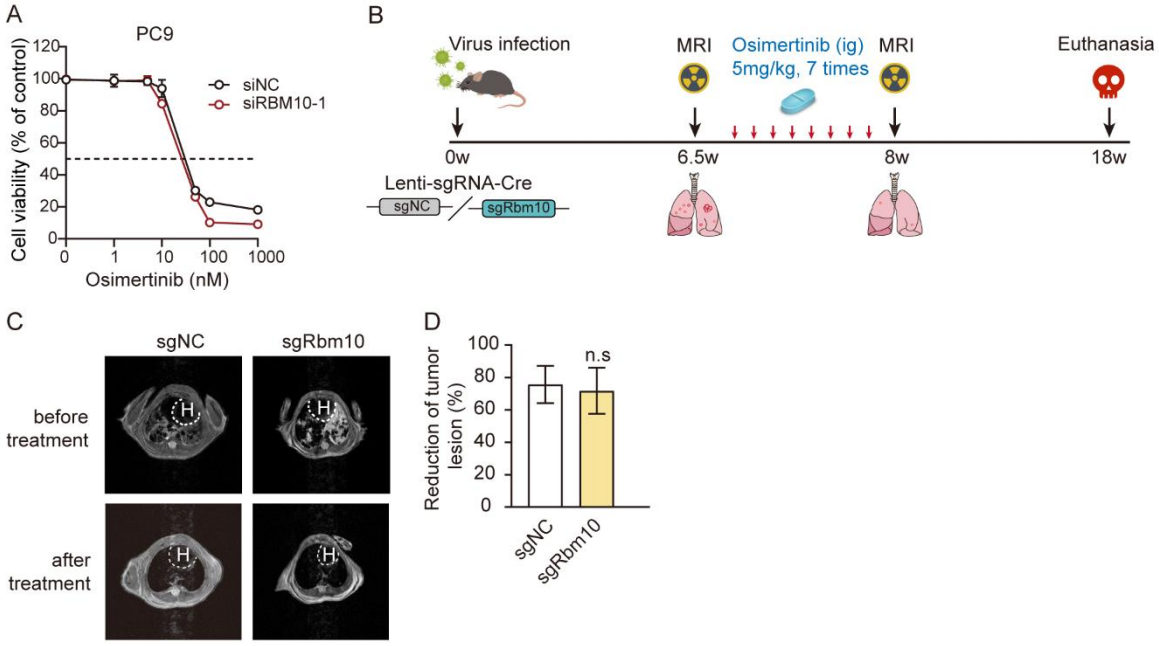

Supplementary Figure S4. Effects of *RBM10* depletion on the efficacy of osimertinib in *EGFR*-mutant LUAD cells and mice tumors. (**A**) Dose response curves of osimertinib in *RBM10*-silenced and control PC9 LUAD cells. n = 4 technical replicates, error bars represent ±SD. (**B**) Experimental scheme of osimertinib treatment in EGFR; Cas9 mouse that were infected with lenti-sgNC-Cre or lenti-sgRbm10-Cre. (**C, D**) Magnetic Resonance Imaging (MRI) detection and quantification of mice tumors before and after osimertinib treatment. H: heart. n = 3, 4 respectively, error bars represent ±SEM. ns: not significant, Student's *t*-test.

Supplementary Fig. S5.

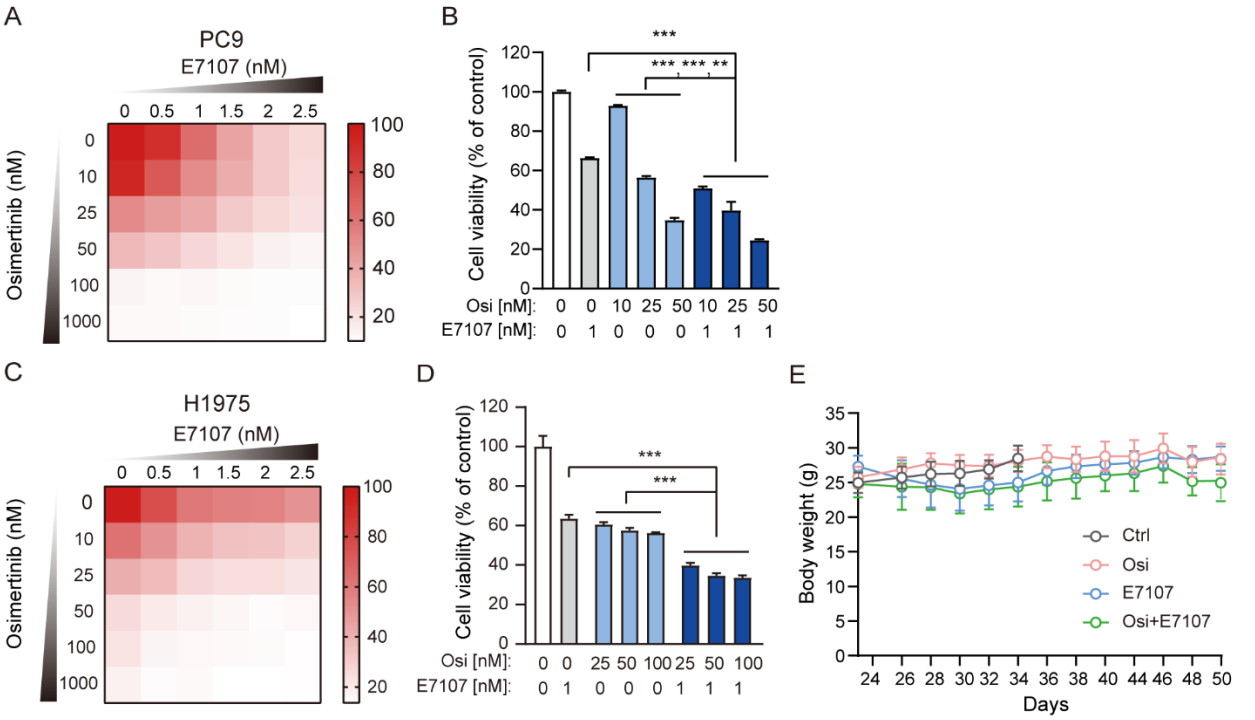

Supplementary Figure S5. *RBM10* deficiency elevates the sensitivity of spliceosome inhibitor in *EGFR*-mutant LUAD cells. (**A**) Heatmap representation and (**B**) bar graphs of the growth of PC9 cells treated with Osi and E7107 individually or in combination. n = 4 technical replicates. (**C**) Heatmap representation and (**D**) bar graphs of the growth of H1975 cells treated with Osi and E7107 individually or in combination. n = 4 technical replicates. (**E**) Mice body weight post drug treatment as indicated in Fig. 5K. n = 5, 6, 6, 6 biological replicates, respectively.
Error bars represent +SD or ±SD in (**B**, **D**), ±SEM in (**E**). ** $P < 0.01$, *** $P < 0.001$, one-way ANOVA followed by Dunnett's tests.

Supplementary Fig. S6.

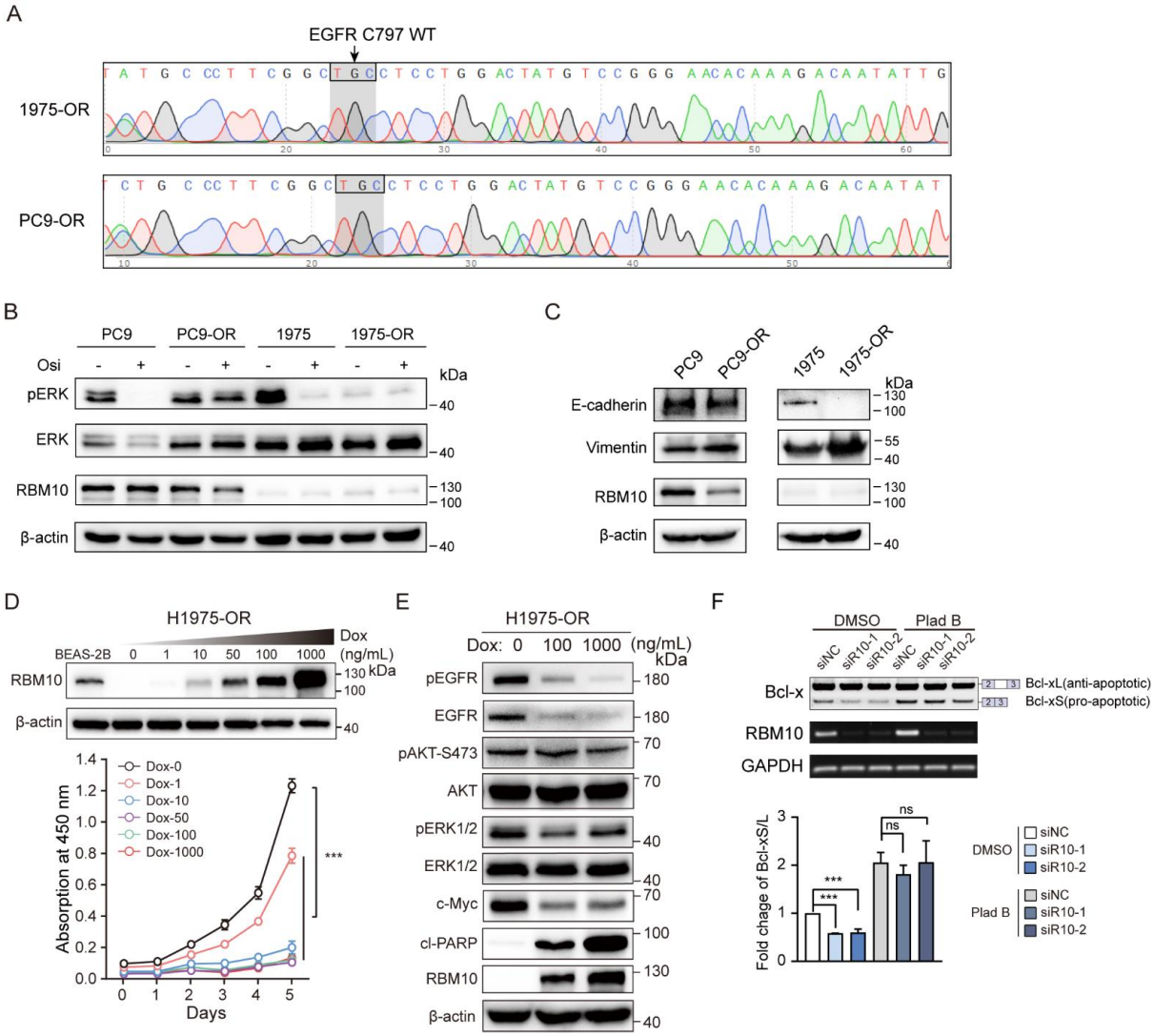

Supplementary Figure S6. Characterization of LUAD cell lines with acquired resistance to osimertinib (PC9-OR and H1975-OR), and splicing changes of Bcl-x induced by *RBM10* knockdown in the absence or presence of Plad B treatment in PC9 cells. (**A**) Sanger sequencing confirms that PC9-OR and H1975-OR do not contain *EGFR* C797 mutation. (**B, C**) Western blot analysis of the bypassing activation of ERK signaling pathway downstream of EGFR (**B**) and marker proteins of epithelial to mesenchymal transition (EMT) (**C**) in PC9-OR and H1975-OR cells. Osimertinib (Osi) added in PC9 and H1975 was 100nM and 1μM, respectively. (**D**) Cell growth of H1975-OR cells following RBM10 re-expression. n = 5 technical replicates. (**E**) Western blot analysis of phosphorylated and total EGFR, AKT, and ERK as well as c-Myc and apoptotic marker proteins under indicated conditions. Loading control: β-actin. (**F**) Splicing changes of Bcl-x in *RBM10*-silenced and control PC9 cells without and with Plad B treatment. PSI: percent-spliced-in. Relative expression of *RBM10* was shown. Loading control: GAPDH.
Error bars represent ±SD in (**D**), ＋SEM in (**F**). *** $P < 0.001$, ns: not significant, two-way ANOVA followed by Bonferroni's tests in (**D**), one-way ANOVA followed by Dunnett's tests were used in (**F**).

Supplementary Tables S1 to S5 (provided as separate excel files)

Supplementary Table S1. Primer and oligonucleotide sequences.

Supplementary Table S2. Gene expression changes induced by *Rbm10* or *Trp53* knockout in mice tumors.

Supplementary Table S3. Splicing changes induced by *Rbm10* knockout in mice tumors.

Supplementary Table S4. Splicing changes associated with *RBM10* loss-of-function mutations in *EGFR*-mutant LUAD samples.

Supplementary Table S5. Splicing changes that are drastically altered by Plad B treatment in *RBM10*-silenced as opposed to control LUAD cells**.**